



## NRC Publications Archive Archives des publications du CNRC

### **Reaction of alkenes with hydrogen-terminated and photooxidized silicon surfaces. A comparison of thermal and photochemical processes**

Mischki, Trevor K.; Donkers, Robert L.; Eves, Brian J.; Lopinski, Gregory P.; Wayner, Danial D. M.

This publication could be one of several versions: author's original, accepted manuscript or the publisher's version. / La version de cette publication peut être l'une des suivantes : la version prépublication de l'auteur, la version acceptée du manuscrit ou la version de l'éditeur.

For the publisher's version, please access the DOI link below. / Pour consulter la version de l'éditeur, utilisez le lien DOI ci-dessous.

#### **Publisher's version / Version de l'éditeur:**

<https://doi.org/10.1021/la060797t>

*Langmuir*, 22, 20, pp. 8359-8365, 2006-08-26

#### **NRC Publications Record / Notice d'Archives des publications de CNRC:**

<https://nrc-publications.canada.ca/eng/view/object/?id=da91e051-e999-4b23-860f-da4ac184c843>

<https://publications-cnrc.canada.ca/fra/voir/objet/?id=da91e051-e999-4b23-860f-da4ac184c843>

Access and use of this website and the material on it are subject to the Terms and Conditions set forth at

<https://nrc-publications.canada.ca/eng/copyright>

READ THESE TERMS AND CONDITIONS CAREFULLY BEFORE USING THIS WEBSITE.

L'accès à ce site Web et l'utilisation de son contenu sont assujettis aux conditions présentées dans le site

<https://publications-cnrc.canada.ca/fra/droits>

LISEZ CES CONDITIONS ATTENTIVEMENT AVANT D'UTILISER CE SITE WEB.

#### **Questions?** Contact the NRC Publications Archive team at

[PublicationsArchive-ArchivesPublications@nrc-cnrc.gc.ca](mailto:PublicationsArchive-ArchivesPublications@nrc-cnrc.gc.ca). If you wish to email the authors directly, please see the first page of the publication for their contact information.

**Vous avez des questions?** Nous pouvons vous aider. Pour communiquer directement avec un auteur, consultez la première page de la revue dans laquelle son article a été publié afin de trouver ses coordonnées. Si vous n'arrivez pas à les repérer, communiquez avec nous à [PublicationsArchive-ArchivesPublications@nrc-cnrc.gc.ca](mailto:PublicationsArchive-ArchivesPublications@nrc-cnrc.gc.ca).



## Reaction of Alkenes with Hydrogen-Terminated and Photooxidized Silicon Surfaces. A Comparison of Thermal and Photochemical Processes

Trevor K. Mischki, Robert L. Donkers, Brian J. Eves, Gregory P. Lopinski, and  
Danial D. M. Wayner\*

Steacie Institute for Molecular Sciences, Nation Research Council, 100 Sussex Drive,  
Ottawa, Ontario, K1A 0R6, Canada, and Chemistry Department, Carleton University,  
1125 Colonel By Drive, Ottawa, Ontario, K1S 5B6, Canada

Received March 24, 2006. In Final Form: June 30, 2006

Reagentless micropatterning of hydrogen-terminated Si(111) via UV irradiation through a photomask has proven to be a convenient strategy for the preparation of ordered bicomponent monolayers. The success of this technique relies upon the differential rate of reaction of an alkene with the hydrogen-terminated and photooxidized regions of the surface. Monolayer formation can be accomplished under either thermal or photochemical conditions. It was observed that, after 3 h, reaction in neat alkene solution irradiation (Rayonet, 300 nm) afforded the expected patterned surface, while thermal conditions (150 °C) resulted in a partial loss of pattern fidelity. Monolayer properties and formation were studied on oxidized and hydrogen-terminated silicon under thermal and photochemical initiation, by contact angle, ellipsometry, Fourier transform infrared spectroscopy, high-resolution electron energy loss spectroscopy, and X-ray photoelectron spectroscopy. Results show that alkenes add to silanol groups on the silica surface in a manner consistent with acid catalysis: once attached to the surface, the silica oxidized the hydrocarbon.

### Introduction

The preparation of hybrid organic–semiconductor devices is an area of growing interest, motivated by applications as diverse as chemical/biological sensor platforms and molecular electronic devices.<sup>1–4</sup> The ability of organic chemistry to provide exquisite control over the properties of the interface between a surface and its environment is well documented; the most studied SAMs being gold–thiol and glass–silane.<sup>5–7</sup> The use of a semiconductor such as silicon as the substrate holds the added benefit that the surface can transduce chemical events at the interface as has been demonstrated for nanowires and oxidized surfaces;<sup>8,9</sup> recent reports have also demonstrated that poly(ethylene glycol)-modified silicon surfaces resist protein binding,<sup>10–12</sup> suggesting that properties originally designed for gold or glass surfaces can be translated to silicon.

Spatial control of the surface chemistry is required for many device applications, and a number of strategies have recently

been reported by us<sup>13</sup> and others.<sup>12,14,15</sup> Our patterning strategy relies on the reactivity difference between oxidized and hydrogen-terminated silicon. Briefly, a hydrogen-terminated silicon wafer is irradiated through a photomask with a UV pen lamp. The shaded regions remain hydrogen terminated, while the illuminated regions are oxidized to form a thin layer of silicon oxide. An alkene then reacts in the hydrogen-terminated regions forming a monolayer-thick organic film. The oxidized portion is then etched with dilute hydrofluoric acid (HF), generating fresh hydrogen-terminated regions ready to react with a second alkene, resulting in a patterned bicomponent monolayer.

Preparation of monolayers containing a minimum of electrically active surface defects is a requirement of any potential device based on this or any patterning strategy. The accepted mechanism for the reaction of alkenes with hydrogen-terminated silicon proceeds via a radical chain reaction as was originally proposed by the Chidsey group<sup>16,17</sup> in their seminal work in this area. While the initial reactions involved pyrolysis of diacyl peroxides, they subsequently reported that the reactions could be initiated by UV irradiation.<sup>18</sup> However, these photochemical reactions were found to lead to significant amounts of oxygen on the surface unless extraordinary measures are taken to exclude dioxygen.<sup>19</sup> This unwanted oxidation reaction is the likely source of electrically active defects observed in electrical measurements of arrays of metal–insulator–semiconductor diodes made via the photooxide patterning method.<sup>20</sup> To improve the electrical

\* Corresponding author. E-mail: Dan.Wayner@nrc.ca.

- (1) Willner, I.; Latz, E. *Angew. Chem., Int. Ed.* **2000**, *39*, 1180.
- (2) de Smet, L. C. P. M.; Stork, G. A.; Hurenkamp, G. H. F.; Sun, Q.-Y.; Topal, H.; Vronen, P. J. E.; Sieval, A. B.; Wright, A.; Visser, G. M.; Zuillhof, H.; Sudhoelter, E. J. R. *J. Am. Chem. Soc.* **2003**, *125*, 13916–13917.
- (3) Roth, K. M.; Yasseri, A. A.; Liu, Z.; Dabke, R. B.; Malinovskii, V.; Schweikart, K.-H.; Yu, L.; Tiznado, H.; Zaera, F.; Lindsey, J. S.; Kuhr, W. G.; Bocian, D. F. *J. Am. Chem. Soc.* **2003**, *125*, 505–517.
- (4) Tomizaki, K. Y.; Usui, K.; Mihara, H. *ChemBioChem* **2005**, *6*, 783–799.
- (5) Koehler, A. N.; Shamji, A. F.; Schreiber, S. L. *J. Am. Chem. Soc.* **2003**, *125*, 8420–8421.
- (6) Ostuni, E.; Chapman, R. G.; Holmin, R. E.; Takayama, S.; Whitesides, G. M. *Langmuir* **2001**, *17*, 5605–5620.
- (7) Yeo, W. S.; Min, D. H.; Hsieh, R. W.; Greene, G. L.; Mrksich, M. *Angew. Chem., Int. Ed.* **2005**, *44*, 5480–5483.
- (8) Zheng, G. F.; Patolsky, F.; Cui, Y.; Wang, W. U.; Lieber, C. M. *Nat. Biotech.* **2005**, *23*, 1294–1301.
- (9) Uslu, F.; Ingebrandt, S.; Mayer, D.; Böcker-Meffert, S.; Odenthal, M.; Offenhäuser, A. *Biosens. Bioelectron.* **2004**, *19*, 1723–1731.
- (10) Clare, T. L.; Clare, B. H.; Nichols, B. M.; Abbott, N. L.; Hamers, R. J. *Langmuir* **2005**, *21*, 6344–6355.
- (11) Perring, M.; Dutta, S.; Arafat, S.; Mitchell, M.; Kenis, P. J. A.; Bowden, N. B. *Langmuir* **2005**, *21*, 10537–10544.
- (12) Bocking, T.; Kilian, K. A.; Hanley, T.; Ilyas, S.; Gaus, K.; Gal, M.; Gooding, J. J. *Langmuir* **2005**, *21*, 10522–10529.

- (13) Wojtyk, J. T. C.; Tomietto, M.; Boukherroub, R.; Wayner, D. D. M. *J. Am. Chem. Soc.* **2001**, *123*, 1535–1536.
- (14) Aizawa, M.; Buriak, J. M. *J. Am. Chem. Soc.* **2005**, *127*, 8932–8933.
- (15) Yang, L.; Lua, Y.-Y.; Lee, M. V.; Linford, M. R. *Acc. Chem. Res.* **2005**, *38*, 933–942.
- (16) Linford, M. R.; Chidsey, C. E. D. *J. Am. Chem. Soc.* **1993**, *115*, 12631–12632.
- (17) Linford, M. R.; Fenter, P.; Eisenberger, P. M.; Chidsey, C. E. D. *J. Am. Chem. Soc.* **1995**, *117*, 3145–3155.
- (18) Terry, J.; Linford, M. R.; Wigren, C.; Cao, R.; Pianetta, P.; Chidsey, C. E. D. *Appl. Phys. Lett.* **1997**, *71*, 1056.
- (19) Cicero, R. L.; Linford, M. R.; Chidsey, C. E. D. *Langmuir* **2000**, *16*, 5688–5695.

properties of the patterned surfaces, we decided to explore monolayer formation using the initially reported thermal approach.<sup>17</sup>

We were surprised to find that, when the SiH/SiO<sub>2</sub> patterned surface was reacted thermally, no contrast was observed between the oxidized and hydrogen-terminated regions based on the surface wetting properties. We anticipated that the alkene would react exclusively in the hydrogen-terminated portion (as it appeared to in the photochemical reaction), but this result suggested that the oxidized portion was also active under the conditions of the thermal reaction. In this paper, we present the results of a comparative study between the reaction of 1-decene with the hydrogen-terminated and oxidized silicon surfaces under either thermal or photochemical initiation. Monolayer formation was followed by water contact angle, ellipsometry, and infrared spectroscopy. The results suggest that the alkene reacts with silanol groups on the oxidized silicon surface under thermal promotion. We show that, although pattern fidelity is lost after the addition of the first alkene, the pattern is merely masked, and the alkyl material present on the oxidized region can be removed by etching with dilute HF, thereby allowing clean reaction of the second monolayer component.

### Experimental Section

**Materials.** Attenuated total reflection (ATR) silicon crystals (25 × 4.5 × 1 mm<sup>3</sup>) were purchased from Harrick, and the silicon wafers were obtained from Virginia Semiconductor. Cleaning and etching solutions were clean-room grade. Sulfuric acid, 96% (H<sub>2</sub>SO<sub>4</sub>), and ammonium fluoride, 40% (NH<sub>4</sub>F), were purchased from J. T. Baker; hydrochloric acid, 30% (HCl) and ammonium hydroxide, 30% (NH<sub>4</sub>OH), were purchased from Olin Microelectronic Materials; hydrogen peroxide, 30% (H<sub>2</sub>O<sub>2</sub>), was purchased from Anachemica; and HF, 48%, was obtained from Arch. MilliQ water (18 MΩ) was used for all experiments. 1-Decene 94% purchased from Aldrich was purified by vacuum distillation at 38–40 °C. Continuously refluxing 1,1,1-trichloroethane (TCE) purchased from Aldrich was used in a Soxhlet Extractor under argon to wash the silicon wafers and ATR elements.

**Surface Characterization.** *Attenuated Total Reflection Fourier Transform Infrared Spectroscopy (ATR-FTIR).* ATR-FTIR spectra were recorded using a Nicolet MAGNA-IR 860 spectrometer at 4 cm<sup>-1</sup> resolution. The ATR crystals were mounted in a purged sample chamber with the light focused normal to one of the 45° bevels. Background spectra were obtained using an oxidized surface.

**Surface Wettability Measurements.** Surface wetting properties were measured with a contact angle goniometer (model: Cam-Micro, Tante, Inc.) under ambient conditions (18–22 °C, 50–60% relative humidity) using a collimated horizontal light beam to illuminate the liquid droplet.

**High-Resolution Electron Energy Loss Spectroscopy (HREELS).** HREELS was carried out under ultrahigh vacuum (UHV) conditions with an LK3000 (LK Technologies) spectrometer. The nominal system resolution was set to 36 cm<sup>-1</sup>. Spectra were acquired in the specular geometry at an incident energy of 6 eV.

**X-ray Photoelectron Spectroscopy (XPS).** XPS spectra were recorded on a PHI 5500 instrument, using monochromated Al Kα (1486 eV) radiation with detection on the surface normal. The pressure during analysis was ~5 × 10<sup>-8</sup> Torr. Spectra were fitted with Gaussian profiles using standard procedures. The positions of all peaks were normalized to C1s at 285.0 eV.

**Thickness Measurements.** The thickness of organic monolayers and silicon oxide were estimated using a Gaertner model L116S single wavelength (633 nm) ellipsometer at an angle of incidence of 70°. The thickness was obtained using a two-layer model with

$n = 1.46$  as the refractive index of the monolayer and silicon oxide, and the silicon substrate was described by  $n = 3.85$  and  $k = 0.02$ .

**Surface Preparation.** *Cleaning and Hydrogen Termination.* Single-sided silicon crystals were used once and discarded; ATR elements were cleaned and reused. All crystals were cleaned with piranha solution (3:1 H<sub>2</sub>SO<sub>4</sub>, 96%/H<sub>2</sub>O<sub>2</sub>, 30%) at 120 °C for 30 min, then rinsed with Milli-Q water. (*Warning: Piranha solutions should be handled with care and kept isolated from organic materials.*) ATR elements were then cleaned with 4:1:1 Milli-Q water/NH<sub>4</sub>OH, 30%/H<sub>2</sub>O<sub>2</sub>, 30% at 80 °C for 15 min, rinsed with Milli-Q water and heated in 4:1:1 Milli-Q water/HCl, 30%/H<sub>2</sub>O<sub>2</sub>, 30% at 80 °C for 15 min then rinsed with Milli-Q water. Samples were hydrogen terminated by etching in degassed ammonium fluoride for 15 min followed by a brief rinse in degassed Milli-Q water.

**Surface Oxidation.** Patterned surfaces were prepared according to our previous work.<sup>13</sup> Irradiation in ambient air of a hydrogen-terminated surface through a photomask (100 μm open squares separated by 50 μm lines; the mask from Adtek is chromium on quartz with an antiscratch coating) with UV light (Hg(Ar) pen lamp, Oriel Model 6035) for 30 min led to the formation of a surface composed of 50 μm Si-H lines and 100 μm oxide squares. The ultraviolet radiation produced by the lamp was dominated by the 254 nm line (~95%), but was also found to contain a weaker 185 nm line (~5%). It is this weaker 185 nm line that has been shown to be responsible for the photochemical oxidation.<sup>21</sup> Unpatterned surfaces were prepared either by irradiation for 30 min from a distance of 2 cm (this has been reported as sufficient to ensure complete oxidation<sup>20</sup>) or by heating in piranha solution for 30 min at 120 °C. Ellipsometry indicated the thickness of the photooxide to be 12 ± 1 Å, while that of the chemical oxide was 10 ± 1 Å.

**Monolayer Formation.** Samples were briefly cleaned using a stream of nitrogen then immersed in deoxygenated 1-decene in a Pyrex Schlenk tube under continuously bubbling argon. The reaction was initiated either via irradiation at 300 nm in a Rayonet photoreactor or thermally at 150 °C for the desired time. The ambient temperature during irradiation was typically 35 °C. The samples were removed from the reaction vessel, washed with TCE in a Soxhlet for 20 min, dried under a stream of nitrogen, and measured. Single-sided wafers were freshly prepared for each time-point, while ATR elements were returned to the reaction vessel. Each FTIR time-point represents the average of at least three ATR elements, the thickness and contact angle measurements represent an average of at least five points on each crystal, and a minimum of two crystals were prepared.

### Results

UV irradiation of a hydrogen-terminated silicon surface through a photomask (50 μm lines spaced 100 μm apart) results in regiospecific oxidation in the exposed regions; after 30 min of irradiation, the pattern can be visualized by exposure to water vapor. The water droplets are centered on the hydrophobic oxide squares (Figure 1A). Thermal reaction of this surface with 1-decene at 150 °C for 90 min results in a loss of contrast between the lines and squares (Figure 1B), indicating that the decene reacts with the oxidized portion of the surface. Photochemical initiation did not result in pattern loss,<sup>13</sup> suggesting that different pathways are available under thermal reaction conditions. In an effort to elucidate the cause of pattern loss, we studied monolayer formation on the photochemically oxidized and hydrogen-terminated silicon surfaces (i.e., not patterned) initiated both thermally and photochemically. It is important to note that the material reacted on the oxidized portion was sensitive to etching by 2% HF and therefore did not affect the ability to form bicomponent monolayers.

The surface wetting properties of H-terminated surfaces reacted with decene were comparable whether prepared via the photochemical (Figure 2A) or thermal (Figure 2B) reaction and achieved

(20) Lopinski, G. P.; Fabre, B.; Wayner, D. D. M. *J. Phys. Chem. B*, submitted for publication, 2006.

(21) Mitchell, S. A. *J. Phys. Chem. B* **2003**, *107*, 9388.



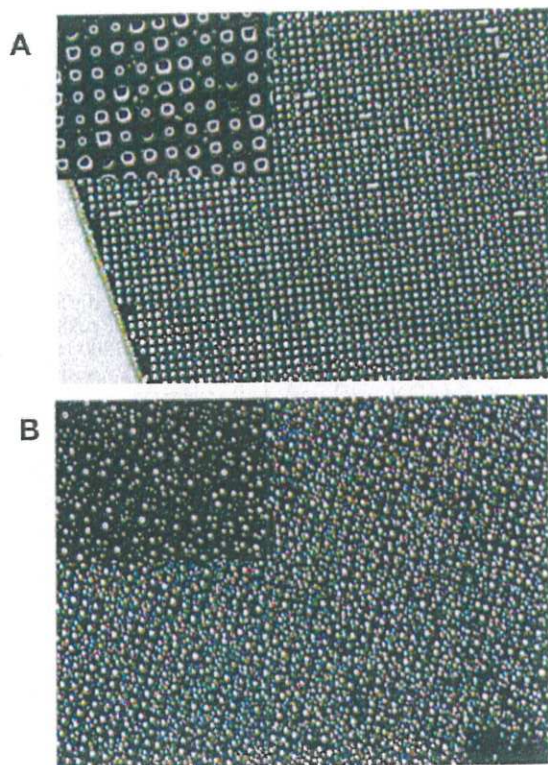


**Figure 1.** Picture of a patterned surface (photomask contains 100  $\mu\text{m}$  lines separated by 100  $\mu\text{m}$ ) exposed to water vapor (A) immediately following photopatterning and (B) after reaction in 1-decene for 90 min at 150  $^{\circ}\text{C}$ .

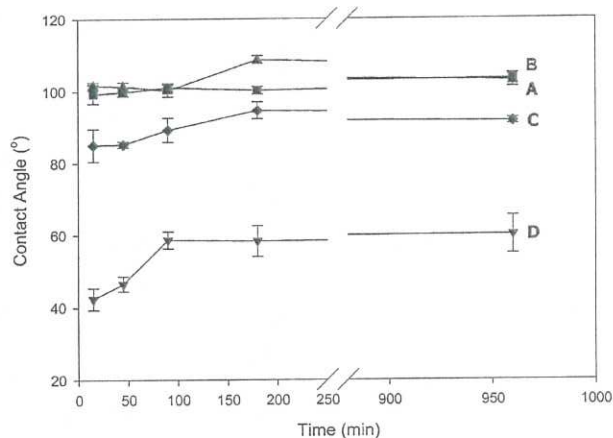


**Figure 2.** Plot of contact angle versus time for the hydrogen-terminated surface reacted (A) thermally and (B) photochemically, and for the photooxide surface reacted (C) thermally and (D) photochemically.

the maximum value ( $102^{\circ}$ ) within 15 min. On the other hand, the wettability of the photooxidized surfaces was highly dependent on the reaction conditions, with the thermal reaction (Figure 2C) producing significantly more hydrophobic surfaces ( $91^{\circ}$ ) than the photochemical reaction (Figure 2D;  $59^{\circ}$ ). The minimal difference ( $\sim 10^{\circ}$ ) between the thermally reacted oxidized surface and the decene-terminated surface is consistent with the loss of contrast in the pattern when tested by exposure to water vapor. An oxidized surface immersed in decene in the dark for 16 h was noticeably more hydrophilic than the photochemically reacted surface. The measured contact angle ( $33^{\circ}$ ) was greater than the

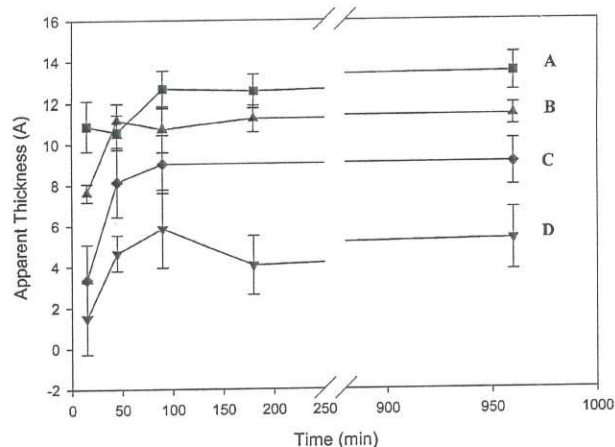


**Figure 3.** Plot of apparent thickness versus time for the hydrogen-terminated surface reacted (A) thermally and (B) photochemically, and for the photooxide surface reacted (C) thermally and (D) photochemically.

initially prepared surface ( $0^{\circ}$ ), suggesting very low inherent reactivity of the oxide surface toward decene.

The thicknesses of the oxide and hydrogen-terminated surfaces were measured at the start of the experiment and subtracted as a background, allowing for a comparison of the alkyl layer thickness. This assumes that the optical properties of the oxide do not change upon addition of an alkyl monolayer. The apparent thickness of the monolayer formed on hydrogen-terminated silicon increases more rapidly for the thermal reaction (Figure 3A) and attains a slightly higher maximum value of  $13.5 \pm 0.9 \text{ \AA}$  compared to the that of the photochemical reaction of  $11.4 \pm 0.5 \text{ \AA}$  (Figure 3B). On the oxidized surface, the thermal reaction (Figure 3C) attains higher coverage ( $9 \pm 1 \text{ \AA}$ ) and a faster rate in comparison with the photochemical reaction (Figure 3D;  $5 \pm 1 \text{ \AA}$ ). Immersion of an oxidized silicon crystal in 1-decene in the dark for 16 h resulted in an apparent thickness of  $2.2 \pm 0.2 \text{ \AA}$ .

During the course of monolayer formation on hydrogen-terminated silicon, the antisymmetric  $\text{CH}_2$  stretching frequency was observed at  $2922 \pm 1 \text{ cm}^{-1}$  throughout the reaction, regardless of the initiation procedure. As evidence of the lower coverage, the antisymmetric methylene stretching frequency of monolayers formed on the oxidized surface was observed at  $2927 \pm 2 \text{ cm}^{-1}$ . Thermal initiation results in a faster rate of reaction on both hydrogen-terminated and oxidized surfaces; after only 10 min, both surfaces reached 80% of the maximum absorbance observed (Figure 4A,C). After 90 min, the photochemical reaction on the hydrogen-terminated surface reached about 90% of its maximum absorbance. The photochemical reaction on the oxide requires a much longer time to reach its maximum (the reaction was stopped after 16 h, although it was not clear that the reaction was complete). The quantity of organic material observed on the oxide surfaces was quite high: after 16 h at 150  $^{\circ}\text{C}$ , the coverage is approximately 40% of that on the hydrogen-terminated surface, and, after 16 h in the photoreactor, the coverage is 25%. Both resulted in more material being deposited than found by immersion of an oxidized ATR crystal in degassed 1-decene for 16 h in the dark at room temperature (22  $^{\circ}\text{C}$ ), which resulted in accumulation equivalent to 4% of the amount on the hydrogen-terminated surface (data not shown).

To gain insight into the mechanism of photooxidation, we used HREELS to follow the process of silicon oxidation under vacuum. A turbo-pumped loadlock of the UHV system, fitted with a sapphire window to facilitate transmission of UV radiation, was used for these experiments. The HREELS spectra after

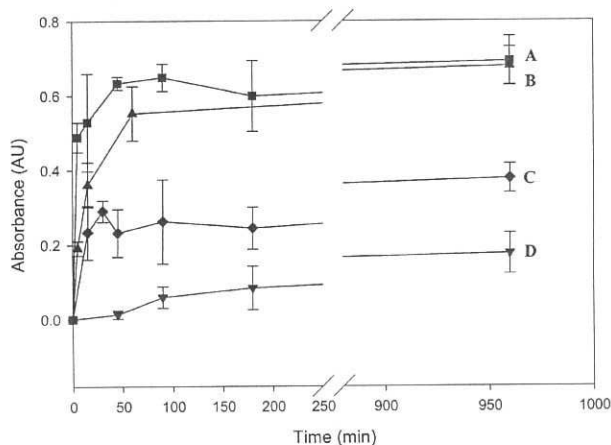


**Figure 4.** Plot of the absorbance of the integrated area of the C–H stretching region ( $2800\text{--}3000\text{ cm}^{-1}$ ) for the hydrogen-terminated surface reacted (A) thermally and (B) photochemically, and for the photooxidized surface reacted (C) thermally and (D) photochemically.

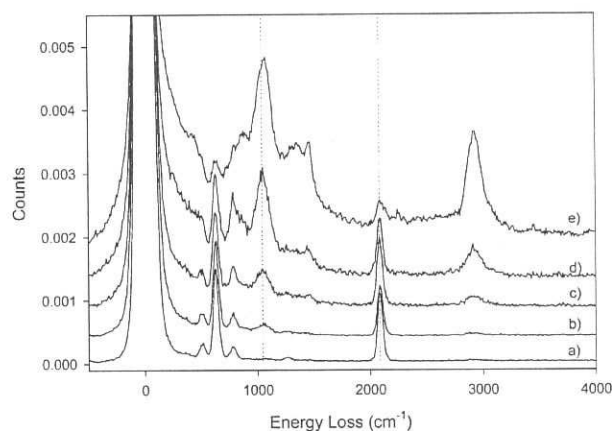


**Figure 5.** HREELS spectrum of hydrogen-terminated silicon (a) before and (b–e) after exposure to 1 Torr of oxygen and UV irradiation for (b) 130 s, (c) 310 s, (d) 20 min and (e) 50 min. All spectra have been normalized to the elastic peak intensity. Spectrum e has been reduced by a factor 2 to fit on the same scale. The vertical dotted lines at  $1045\text{ cm}^{-1}$  and  $2085\text{ cm}^{-1}$  indicate the position of the Si–O–Si and Si–H modes, respectively.

exposing a hydrogen-terminated silicon surface to 1 Torr of oxygen under UV irradiation are shown in Figure 5. The as-prepared H-terminated Si(111) surface exhibits characteristic peaks at  $635$  and  $2084\text{ cm}^{-1}$  due to the Si–H bend and stretch modes, respectively, as well as weaker peaks at  $510\text{ cm}^{-1}$  and  $780\text{ cm}^{-1}$ , which have been attributed to Si substrate phonon modes.<sup>22,23</sup> Exposure of this surface to 1 Torr of  $\text{O}_2$  for 30 min in the absence of UV irradiation did not result in any significant changes to this vibrational spectrum. However, when the surface was exposed to oxygen under irradiation with the Hg pen lamp, exposure times as short as 1 min led to irreversible changes in the spectrum, most notably a decrease in the elastic peak intensity and growth of a peak at  $1045\text{ cm}^{-1}$  attributed to the Si–O–Si stretch mode.<sup>24,25</sup> For longer exposures, this mode continues to increase in intensity. For a 50 min exposure, this mode is observed to shift up to  $1070\text{ cm}^{-1}$  and is also accompanied by modes at

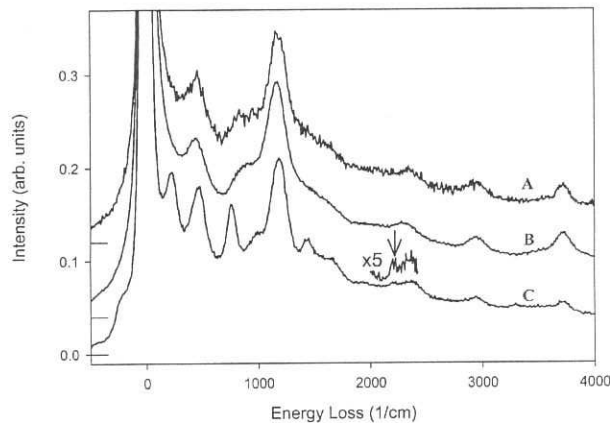


**Figure 6.** HREELS spectra (normalized to the elastic peak) of H/Si(111) oxidized by (A) piranha solution, (B) nitric acid, and (C) irradiation in air. For spectrum C, the region between  $2000$  and  $2450\text{ cm}^{-1}$  has been magnified by a factor of 5, with the arrow indicating the weak peak at  $2230\text{ cm}^{-1}$  attributed to residual Si–H bonds. The feature at  $2360\text{ cm}^{-1}$  is an overtone of the  $1180\text{ cm}^{-1}$  peak.

$460\text{ cm}^{-1}$  and  $860\text{ cm}^{-1}$ , which can also be assigned to oxygen inserted into Si–Si back-bonds.<sup>24</sup> For exposures up to 30 min, the Si–H stretch mode remains relatively sharp, with only a slight broadening on the higher energy side. This mode is expected to shift upward as oxygen is inserted into the Si–Si back-bonds. Shifts of this mode to  $2110\text{ cm}^{-1}$ ,  $2160\text{ cm}^{-1}$ , and  $2250\text{ cm}^{-1}$  have been attributed to the Si–H stretch with one, two, and three oxygens in the back-bond, respectively.<sup>25,26</sup> After 50 min of exposure, the sharp Si–H mode is seen to broaden significantly, and a new peak is resolved at  $2250\text{ cm}^{-1}$ , indicative of regions of complete oxygen insertion (i.e.,  $\text{O}_3\text{--Si--H}$ ). It is interesting to note that, even after this extended exposure, no silanol (Si–OH) modes at  $3720\text{ cm}^{-1}$  are observed. This suggests that surface oxidation proceeds via the insertion of oxygen into the silicon back-bonds (either direct insertion or through a pentavalent intermediate), and not the silicon–hydrogen bond. This process is presumably thermodynamically driven since it results in the formation of two silicon–oxygen bonds. We also note the large increase in the C–H stretch mode intensities at  $2920\text{ cm}^{-1}$ , signifying a considerable level of hydrocarbon contamination. This likely results from gas-phase photochemical reactions of organic contaminants in the loadlock, resulting in the covalent attachment of hydrocarbons to the surface. Similar gas-phase reactions have recently been reported to be quite efficient under UV initiation.<sup>27</sup>

It is interesting to contrast the more controlled vacuum photochemical oxidation process with surfaces photooxidized in lab air or thermally oxidized in solution, which are, in fact, the relevant oxidized surfaces whose reactivity is the subject of the current study. HREELS spectra of silicon surfaces oxidized with piranha solution ( $120\text{ }^\circ\text{C}$  for 20 min, Figure 6A) or nitric acid ( $80\text{ }^\circ\text{C}$ , Figure 6B) exhibit rather similar spectra, characterized by strong peaks at  $450$  and  $1180\text{ cm}^{-1}$ . These spectra are similar to that previously reported for thin  $\text{SiO}_2$  films.<sup>28</sup> The  $1180\text{ cm}^{-1}$  mode corresponds to the surface optical phonon or Fuchs Kliever mode and corresponds well with the calculated value based on IR observations of the LO and TO phonons in ultrathin ( $\sim 1\text{ nm}$ )  $\text{SiO}_2$  films.<sup>29</sup> The presence of surface silanol groups is clearly

(22) Dumas, P.; Chabal, Y. J. *Chem. Phys. Lett.* **1991**, *181*, 537.

(23) Stuhlmann, Ch.; Bogdányi, G.; Ibach, H. *Phys. Rev. B* **1992**, *45*, 6786.

(24) Ikeda, H.; Nakagawa, Y.; Toshima, M.; Furuta, S.; Zaima, S.; Yasuda, Y. *Appl. Surf. Sci.* **1997**, *117/118*, 109.

(25) Weldon, M. K.; Stefanov, B. B.; Raghavachari, K.; Chabal, Y. J. *Phys. Rev. Lett.* **1997**, *79*, 2851.

(26) Schaeffer, J. A.; Frankel, D.; Stucki, F.; Gopel, W.; Lapeyre, G. J. *Surf. Sci.* **1984**, *139*, L209.

(27) Eves, B. J.; Lopinski, G. P. *Langmuir* **2006**, *22*, 3180.

(28) Wang, S. D.; Dong, X.; Lee, C. S.; Lee, S. T. *J. Phys. Chem. B* **2005**, *109*, 9892.



indicated by the appearance of O–H stretch modes at  $3720\text{ cm}^{-1}$ . The shoulder at  $\sim 850\text{ cm}^{-1}$  reflects contributions from the Si–O–H stretch mode as well as modes of the oxide. There is no evidence of a Si–H peak; the weak feature at  $2360\text{ cm}^{-1}$  can be assigned to the overtone of the  $1180\text{ cm}^{-1}$  mode. For a surface that was photooxidized in air for 30 min (Figure 6C), the spectrum is somewhat different. The main oxide peaks are still present, although the lower frequency peak is shifted up to  $470\text{ cm}^{-1}$ . Two additional modes at 225 and  $760\text{ cm}^{-1}$  are observed, which are not apparent on the chemically oxidized samples. Another noticeable difference is the reduced intensity of the  $3720\text{ cm}^{-1}$  mode, indicating a decreased number of silanol groups relative to the samples prepared in solution. A weak peak at  $2230\text{ cm}^{-1}$  can be assigned to Si–H with oxygen inserted into all three silicon–silicon back-bonds ( $\text{O}_3\text{–Si–H}$ ), suggesting that, in contrast to the chemical oxidation processes, not all Si–H bonds have been removed. In summary, the HREELS spectra indicate that the photo- and chemically oxidized surfaces have a similar structure, although the latter exhibits some residual Si–H groups and correspondingly fewer hydroxyl moieties. Comparing the spectra after air oxidation versus that under oxygen in a vacuum, it is apparent that the former is considerably more rapid, perhaps suggesting a role for water in accelerating the photooxidation reaction.

The final characterization performed was XPS on a freshly photooxidized silicon sample and oxide samples reacted thermally and photochemically for 90 min. The C1s region on the oxide reference sample shows unshifted carbon at 285 eV, an ether linkage at 286.5 eV, and a small amount of acid/ester at 289 eV (Figure 7A). Potential sources of this adventitious hydrocarbon contamination include deposition during photooxidation, which was conducted under ambient conditions with a UV pen lamp and generated ozone, which, in turn, may have induced the formation of reactive intermediates that may have deposited on the surface. The photochemically reacted surface shows only a small accumulation of organic material, (Figure 7B) consistent with the contact angle, ellipsometry and FTIR results. The increase in the ether feature is consistent with hydrocarbons attached via a Si–O–C link, although the ratio of ether to unshifted carbon is much larger than expected based on decyl chains attaching to the surface. In contrast, the surface reacted thermally (Figure 7C, 90 min at  $150^\circ\text{C}$ ) indicates a much larger amount of hydrocarbon on the surface. Decomposing the observed spectrum into the various components yields an ether-to-methylene carbon ratio of  $\sim 1:10$ , close to that expected for decyl chains bound to the surface via a Si–O–C link. The spectrum also indicates the presence of a significant amount of carbon in higher oxidation states, including the acid/ester at 289.5 eV and a weak ketone-related feature at 288 eV. The presence of oxidized hydrocarbon is unique to the oxide surfaces; as we have shown, 1-decene reacted with the hydrogen-terminated results in a single C1s peak in the XPS.<sup>30</sup> The origin of the oxidized material is a topic currently under investigation in our lab but is reminiscent of hydrocarbon cracking using acidic zeolite catalysts.

### Discussion

Upon confirming that the unexpected loss of pattern after thermal initiation was due to decene reacting with the oxide surface, a model was developed centered on inhomogeneous oxidation of the hydrogen-terminated silicon surface. Initially,

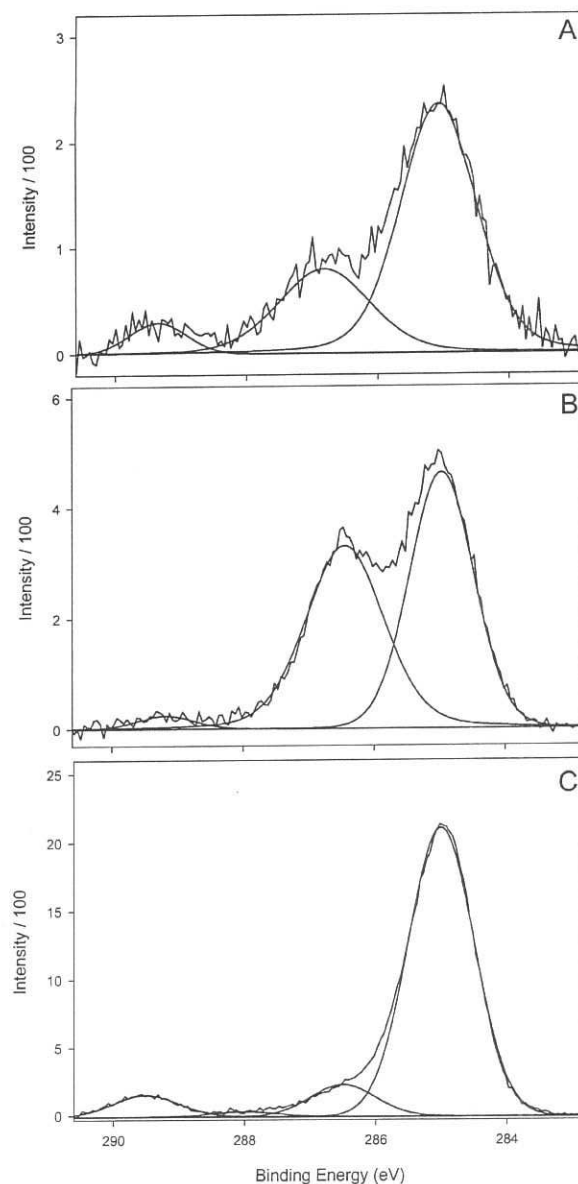


**Figure 7.** High resolution XPS spectrum of the C1s region for (A) the photooxidized surface, (B) the surface obtained following photochemically initiated reaction of decene with the oxide surface, and (C) the surface obtained following thermal reaction with the oxide surface.

we hypothesized that, after photooxidation under ambient conditions, the surface resulted in incomplete oxidation of the surface, which would be composed of a mixture of  $\text{O}_n\text{Si–H}$  and  $\text{O}_3\text{SiOH}$  regions since the HREELS indicated the presence of unshifted Si–H after exposure to oxygen in a vacuum. On such a surface, decene was expected to react under both photochemical and thermal initiation with the unoxidized regions. The additional material reacted under thermal initiation was postulated to be derived from reaction on the partially oxidized region. This model was consistent with wettability data, ellipsometric thickness, and FTIR measurements. However, in comparing the HREELS spectra of surfaces after chemical or ambient photooxidation, it was apparent that they were not very different (apart from the presence of a small number of  $\text{O}_3\text{–Si–H}$  moieties on the photooxidized surface). To determine whether these groups were responsible for the attachment of decene, the reactivity of chemically oxidized

(29) Queeney, K. T.; Weldon, M. K.; Chang, J. P.; Chabal, Y. J.; Gurevich, A. B.; Sapjeto, J.; Opila, R. L. *J. Appl. Phys.* **2000**, *87*, 1322.

(30) Boukherroub, R.; Morin, S.; Bensebaa, F.; Wayner, D. D. M. *Langmuir* **1999**, *15*, 3831–3835.

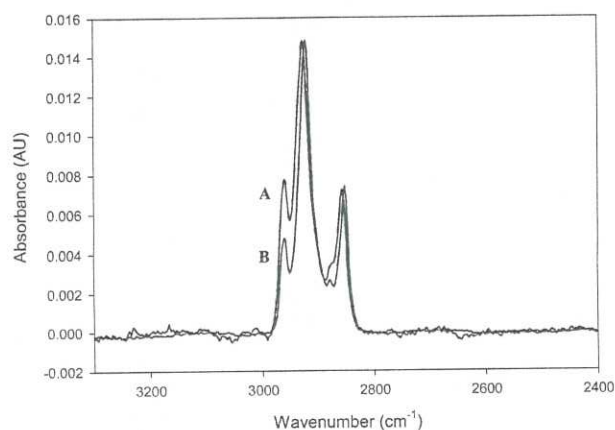


**Figure 8.** ATR-FTIR spectrum of decene reacted with (A) the oxidized surface and (B) the hydrogen-terminated silicon surface, expanded in the C–H stretching region and normalized to the absorbance maximum.

**Table 1.** Ratio of the Area of the Antisymmetric Methyl Stretch to the Antisymmetric Methylene Stretch on Hydrogen-Terminated and Oxidized Surfaces Prepared under Different Initiation Conditions

surface termination	thermal (150 °C)	thermal (80 °C)	photochemical (300 nm)
Si–H	0.20 ± 0.01		0.20 ± 0.02
Si–O	0.32 ± 0.02	0.37 ± 0.05	0.39 ± 0.05

surfaces were studied. Piranha-oxidized silicon wafers were found to thermally react with decene at 150 °C in a manner similar to that observed on the photooxidized surfaces. Even piranha-cleaned glass microscope slides were observed to react with 1-decene; after 16 h at 150 °C, the surface was observed to be hydrophobic with a contact angle of 87°. These experiments confirmed that the reactivity of the alkene with the photooxidized surface was not due to residual Si–H modes but rather a more general property of SiO<sub>2</sub> surfaces. Coupled with the XPS data, which shows evidence for ether linkages, this implicates the silanol groups as likely reactive sites.

Further analysis of the FTIR spectra sheds light on the mechanism of alkene reaction with the oxidized surface. It is important to note that the ratio of methyl to methylene absorbance (e.g., comparing the integrated absorbance of the antisymmetric modes) is greater from the reactions with the oxide surface compared to those with the hydrogen-terminated surface (Table 1). This could be consistent with Markonikoff addition since the FTIR spectra would show an increase in methyl groups relative to methylene groups. A report of the addition of 2,4,4-trimethyl-1-pentene to a silica–alumina surface under UHV conditions at –63 °C provides support for this suggestion. In this case, addition

to the silanol occurred exclusively at the 2 position of the alkene.<sup>31</sup> The more acidic zeolite surface presumably allows the reaction to proceed at lower temperatures. Radical-mediated addition of an alkene to the hydrogen-terminated surface is known to result in addition at the 1 position, while addition to the silanol was expected to occur at both the 1 and 2 positions. Indeed, the peak area of the antisymmetric methyl stretch (2960 cm<sup>–1</sup>) relative to the antisymmetric methylene stretch (2922 cm<sup>–1</sup>) was higher on the oxidized surface (Figure 8, Table 1). The ratio was highest when the reaction was performed at lower temperatures (thermally at 80 °C or at room temperature photochemically) and is consistent with a thermally activated process favoring Markonikoff addition at lower temperatures. The ratio did not change during the course of the reaction, and, at 80 °C after 16 h, the total coverage was 18% of the maximum coverage achieved on the hydrogen-terminated surface (data not shown).

It is clear at this time that photochemical initiation of the reaction results in the addition of more organic material to the surface than when left in the dark at room temperature (25 versus 4% relative to a complete decyl-terminated monolayer) and in approximately the same amount as when the reaction is conducted thermally at 80 °C (18% of a complete monolayer). The reason behind the enhanced reactivity is not understood at this time, but is likely a result of an acid-catalyzed process by the silanol groups at the surface. The presence of oxidized hydrocarbon species attached to the surface, detected by XPS, suggests that the surface may be catalytically active; a process known for more acidic substrates such as metal-doped silica or silica–alumina.<sup>32,33</sup> A greater understanding of this process is required to limit unwanted side products that may have an impact on the electrical performance of a device.

This current report provides a more complete understanding of our original observations.<sup>13</sup> Previously, we reported that scanning auger electron spectroscopy of a patterned surface after reaction with 1-decene photochemically showed contrast between oxidized and alkyl regions. However, in the oxidized region, the carbon signal indicated the presence of a low level of carbonaceous material. This was initially attributed to adventitious, physisorbed carbon contamination. We now believe this to be the result of 1-decene covalently bonded to the oxidized surface. This is supported by the XPS spectrum in Figure 7B as well as the thickness and FTIR data in Figures 2 and 3. Although the total amount of hydrocarbon by XPS is much lower on the “photochemically initiated” reactions, there is evidence for SiO–C bonding and a much smaller amount of carbonyl compared to Figure 7C. The much slower reaction under the photochemical conditions is consistent, not with a photoactivated process, but with a slow thermally activated process (35 °C).

Since the organic material is bound to the oxidized region via SiO–C bonds, it is chemically sensitive to HF and can be

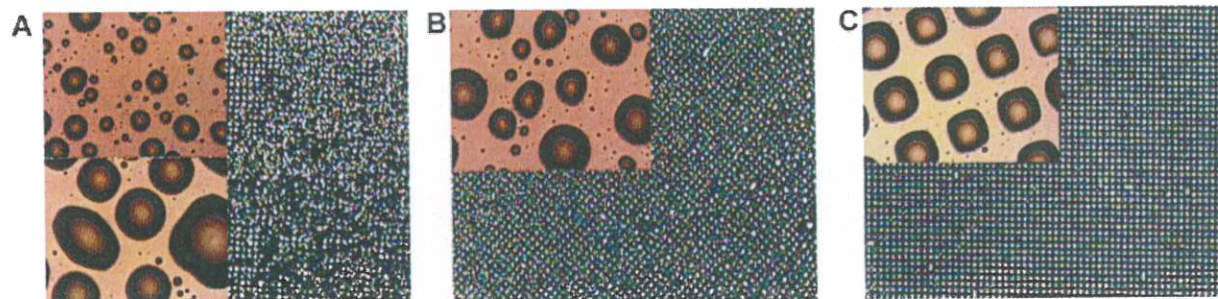


**Figure 9.** Picture of a photopatterned oxide surface exposed to water vapor after (A) 18 h in 1-decene at 150 °C, followed by (B) immersion in 2% HF for 2 min, then (C) UV oxidation, demonstrating the reemergence of a sharp pattern.

selectively removed, leaving newly formed hydrogen-terminated silicon. Figure 9B shows the pattern partially restored after immersion in 2% HF following thermal reaction of the oxide-patterned surface with 1-decene. A second brief photooxidation fully restores the pattern fidelity (Figure 9C). As an additional note, it is expected that, to derivatize the oxide using alkoxy/chloro silane chemistry, the initial oxide will have to be etched to remove accumulated alkyl material and reoxidized to provide a surface free from organic contamination.

### Conclusions

We have shown that photooxidation of Si-H (111) under ambient lab conditions leads to the formation of a SiO<sub>2</sub> surface

layer that is spectroscopically and functionally similar to a chemically oxidized surface. The resulting oxide surface reacts thermally (150 °C) and photochemically (Rayonet photoreactor) with 1-decene to provide a partial alkyl monolayer. This is consistent with the addition of alkene to the silanol surface via Markonikoff addition to the silanol in an acid-catalyzed process. The increased methyl-to-methylene ratio at 150 °C compared to 35 °C is consistent with a competing anti-Markonikoff addition at higher temperatures, although other possibilities cannot not be ruled out unequivocally. For example, XPS indicates the presence of oxidized hydrocarbon on the surface after thermal reaction, indicating that other reaction pathways lead to the oxidative degradation of the films. Further work will be conducted to elucidate the nature of this reactivity.

**Acknowledgment.** We thank G. I. Sproule and Simona Moisa (NRC-IMS) for the XPS measurements and Doug Moffatt and Mauro Tomietto (NRC-SIMS) for valuable technical assistance.

LA060797T

(31) Ishikawa, H.; Yoda, E.; Kondo, J. N.; Wakabayashi, F.; Domen, K. *J. Phys. Chem. B* **1999**, *103*, 5681–5686.

(32) Babbitz, S. M.; Williams, B. A.; Miller, J. T.; Snurr, R. Q.; Haag, W. O.; Kung, H. H. *Appl. Catal., A* **1999**, *179*, 71–86.

(33) Narbeshuber, T. F.; Brait, A.; Seshan, K.; Lercher, J. A. *J. Catal.* **1997**, *172*, 127–136.